Stem Cell Reports
Report
OPEN ACCESS

Genome Toxicity and Impaired Stem Cell Function after Conditional Activation of CreER^{T2} in the Intestine

Natacha Bohin,[1,2] Elizabeth A. Carlson,[1] and Linda C. Samuelson[1,2,*]
[1]Department of Molecular & Integrative Physiology, University of Michigan, Ann Arbor, MI 48109, USA
[2]Cellular & Molecular Biology Graduate Program, University of Michigan, Ann Arbor, MI 48109, USA
*Correspondence: lcsam@umich.edu
https://doi.org/10.1016/j.stemcr.2018.10.014

SUMMARY

With the tamoxifen-inducible CreER^{T2} system, genetic recombination can be temporally controlled in a cell-type-specific manner in intact animals, permitting dissection of the molecular underpinnings of mammalian physiology. Here we present a significant drawback to CreER^{T2} technology for analysis of intestinal stem cells. Using the intestine-specific *Villin-CreER^{T2}* mouse strain, we observed delayed intestinal regeneration post irradiation. *Villin-CreER^{T2}* activation was associated with DNA damage and cryptic *loxP* site cleavage. Analysis of stem cell-specific CreER^{T2} strains showed that the genome toxicity impairs function of crypt base columnar stem cells, resulting in loss of organoid initiating activity. Importantly, the stem cell impairment is short-lived, with return to normal by 7 days post tamoxifen treatment. Our findings demonstrate that mouse genetic experiments that utilize CreER^{T2} should consider the confounding effects of enhanced stem cell sensitivity to genome toxicity resulting from CreER^{T2} activation.

INTRODUCTION

The Cre-*loxP* system is a powerful genome-editing tool that revolutionized *in vivo* genetic studies. The site-specific Cre recombinase catalyzes recombination between two 34-bp *loxP* DNA recognition sites to induce deletion or activation of target transgenes (Bouabe and Okkenhaug, 2013). The adaptation of this system from its bacteriophage origin requires that Cre and *loxP* be engineered into the mouse genome. Since the mouse genome does not contain *loxP* sites, recombination is designed to be specific to the engineered target construct.

One advance to the Cre-*loxP* system was the development of inducible Cre by fusion with a mutated ligand-binding domain of the estrogen receptor (Metzger et al., 1995). The CreER recombinases (e.g., CreER^{T2}) are activated by the estrogen receptor antagonist tamoxifen (TX), which allows temporal control of target gene rearrangement. In the absence of TX, CreER is cytoplasmic. TX binding induces CreER transfer into the nucleus to catalyze recombination between *loxP* sites. The recombined allele is a permanent genetic change. Thus, this system has been a powerful tool to study adult stem cell function. In particular, there are numerous CreER mouse strains used to study intestinal stem cells (ISCs), including *Villin-CreER^{T2}* (el Marjou et al., 2004), which is expressed throughout the intestinal epithelium, including stem and progenitor cells, and ISC-specific *Olfm4-CreER^{T2}* (Schuijers et al., 2014) and *Lgr5-CreER^{T2}* (Barker et al., 2007).

Off-target recombination has been observed at cryptic *loxP* (*cloxP*) sites, which have DNA sequence similarity to *loxP* (Thyagarajan et al., 2000). The consequences of illegitimate Cre recombination vary from cellular toxicity to overt developmental and pathological defects. Cre expression in developing spermatids led to male sterility due to genomic rearrangements (Schmidt et al., 2000), and widespread developmental defects occurred after TX activation of CreER^{T2} during embryonic development (Naiche and Papaioannou, 2007). CreER^{T2} genotoxicity in proliferating adult tissues has also been described, with TX-activated CreER^{T2} causing epithelial atrophy and metaplasia in stomach (Huh et al., 2010), and chromosomal rearrangements in immature hematopoietic cells (Higashi et al., 2009). These reports suggest that proliferating stem and progenitor cells may be particularly sensitive to Cre-mediated genotoxicity, although this has not been tested in most adult stem cell populations.

One of the most proliferative adult tissues is the intestine, where adult stem cells fuel rapid epithelial cell turnover. Whether off-target DNA cleavage and genotoxicity are an issue for ISC Cre drivers has not been reported. In this study we observed functional ISC defects following TX induction of CreER^{T2} in the mouse intestine. Whole-body γ-irradiation subsequent to *Villin-CreER^{T2}* activation resulted in delayed intestinal regeneration. ISC defects were demonstrated by impaired organoid-forming efficiency. Our findings suggest that the flood of TX-activated CreER^{T2} into the nucleus leads to cleavage at c*loxP* sites and DNA double-stranded breaks (DSBs), which impair ISC function. Thus, this study holds significant implications for experiments studying intestinal homeostasis and regeneration in mouse genetic models to mitigate CreER^{T2} toxicity in ISCs.

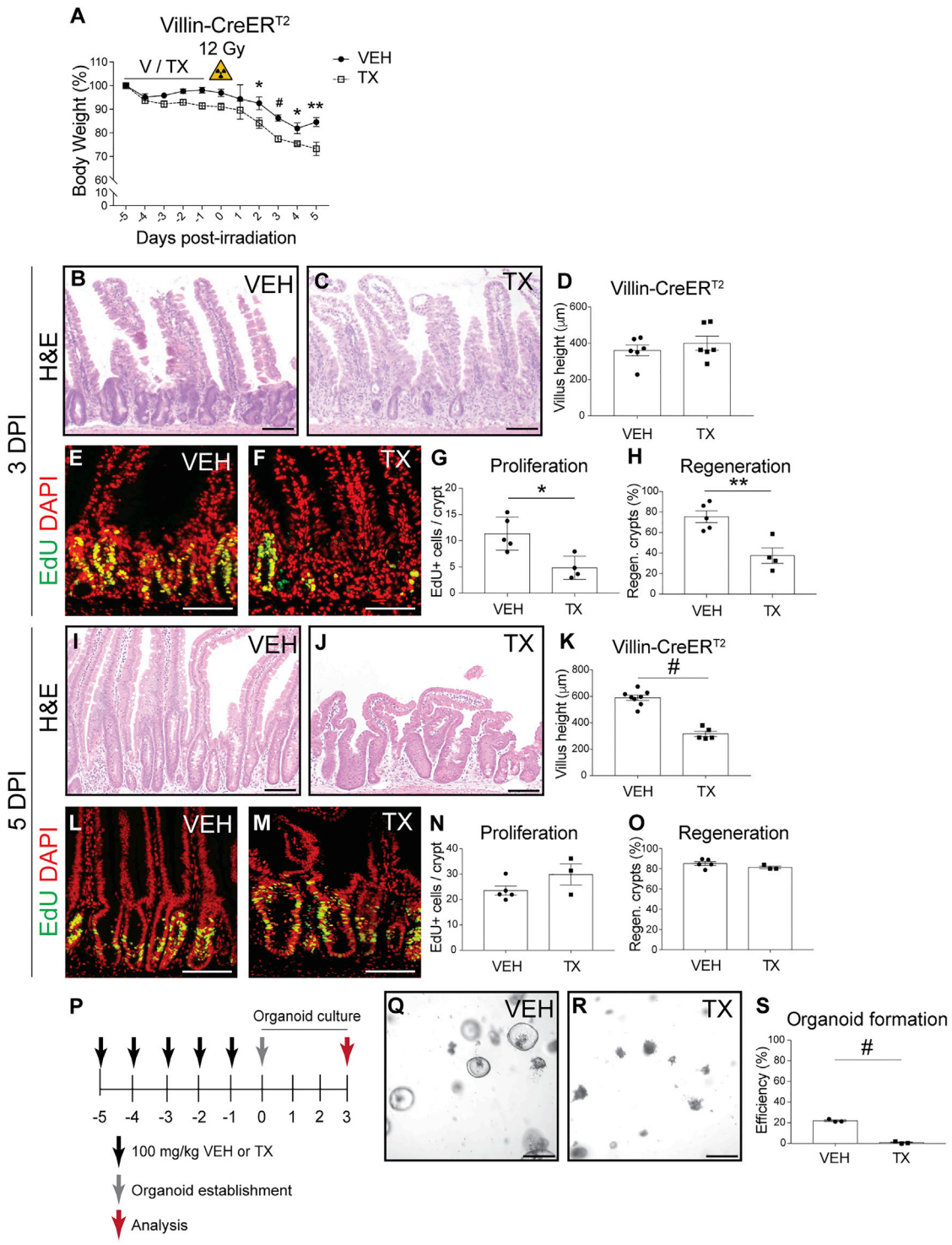

Figure 1. Impaired Intestinal Regeneration and Organoid Formation in TX-Treated *Villin-CreER^{T2}* Mice

(A–O) *Villin-CreER^{T2}* mice were treated with TX (100 mg/kg) or vehicle (V; also VEH) daily for 5 days, and 1 day later either (A–O) challenged with 12 Gy γ-irradiation or (P–S) tested for organoid-forming efficiency. (A) Mouse body weight relative to weight at the initiation of treatment (n = 7–15 mice/group). (B–O) Duodenal crypt regeneration was assessed at (B–H) 3 days post irradiation (DPI) and (I–O) 5 DPI by (B, C, I, and J) H&E staining, and (E, F, L, and M) EdU incorporation. (D and K) Villus height (n = 5–8 mice/group), (G and N) cellular proliferation, and (H and O) crypt regeneration were measured (n = 4–5 mice/group).

(legend continued on next page)

RESULTS

Impaired Intestinal Regeneration in *Villin-CreER^{T2}* Mice

We tested the effect of *Villin-CreER^{T2}* on ISC function after treatment with TX (100 mg/kg) or vehicle (VEH). Histological analysis did not reveal any gross intestinal changes induced by TX treatment; tissue architecture and cellular proliferation did not differ from controls (Figure S1). However, marked differences were observed between TX- and VEH-treated *Villin-CreER^{T2}* mice after challenge with 12 Gy irradiation (Figure 1). TX-treated mice had a more pronounced post-irradiation weight loss compared with controls (Figure 1A), and histological analysis showed more extensive intestinal damage (Figures 1B–1O). Three days post irradiation (DPI), the intestines of VEH-treated mice began to recover with a typical regenerative response, characterized by expanded crypts and increased proliferation (Figures 1B and 1E). In contrast, TX-treated mice had extensive decellularized crypts and very few, small crypt structures (Figure 1C). We also observed decreased proliferation and fewer regenerating crypts in the TX group (Figures 1G and 1H). At 5 DPI, the villi of TX-treated *Villin-CreER^{T2}* mice were blunted, consistent with impaired regeneration at 3 DPI (Figures 1I–1K). However, crypts at this time point were undergoing robust regeneration, similar to control (Figures 1L–1O). Thus, TX activation of *Villin-CreER^{T2}* results in delayed intestinal regeneration, consistent with enhanced damage following 12 Gy irradiation.

Impaired Organoid Formation after *Villin-CreER^{T2}* Activation

To understand the basis for the altered response of *Villin-CreER^{T2}* mice to irradiation, we tested if CreER^{T2} activation affects ISC function by measuring organoid-forming efficiency in unirradiated, treated mice. Duodenal crypts were isolated from TX- or VEH-treated mice 1 day post treatment, and cultured under conditions that support ISC growth (Figure 1P). While crypts isolated from VEH-treated mice grew into typical spheroids by 3 days in culture, crypts isolated from TX-treated *Villin-CreER^{T2}* mice exhibited very poor organoid growth (Figures 1Q and 1R). Quantification showed that 25-fold fewer organoids grew in cultures initiated from TX-treated mice than VEH-treated mice (Figure 1S). The extreme loss of organoid-forming activity in TX-activated *Villin-CreER^{T2}* mice suggests impaired ISC function.

Impaired ISC Function Is Not due to TX Toxicity

We tested whether the delayed regenerative response to irradiation and the impaired organoid-forming efficiency were due to TX toxicity, which has been observed in other studies (Huh et al., 2012; Zhu et al., 2013). Irradiated, non-transgenic C57BL/6 mice treated with TX or VEH had similar changes to body weight and intestinal histology, including villus height, proliferation rate, and crypt regeneration (Figures S2A–S2H). Further, TUNEL staining and organoid-forming efficiency did not differ between the two groups (Figures S2I–S2K). These data showed that toxicity caused by TX treatment of *Villin-CreER^{T2}* mice was not a direct effect of TX.

Next, we determined whether the TX effect on Cre recombinase was independent of CreER-mediated nuclear translocation. We treated *Villin-Cre* mice, which exhibit constitutive Cre expression in intestinal epithelial cells (Madison et al., 2002), with TX or VEH, followed by 12 Gy irradiation. In contrast to the response in *Villin-CreER^{T2}* mice, we saw no heightened sensitivity to irradiation in TX-treated *Villin-Cre* mice (Figures S2L–S2S). Further, there was no change in TUNEL staining or organoid-forming efficiency (Figures S2T–S2V). Notably, these transgenic strains express similar amounts of Cre protein, so the toxicity is not due to higher levels of Cre recombinase expression in *Villin-CreER^{T2}* mice (Figure S2W). Together these results support the conclusion that TX activation of *Villin-CreER^{T2}* mediates impaired intestinal regeneration and organoid formation, and not TX toxicity, or interactions between TX and constitutively active Cre recombinase.

Impaired Organoid Formation after CreER^{T2} Activation in ISCs

Heightened sensitivity to radiation and impaired organoid-forming capacity of *Villin-CreER^{T2}* mice after TX treatment suggested that CreER activation induced stem cell damage. We tested ISC-specific CreER^{T2} mouse strains that target crypt base columnar (CBC) ISCs, including *Olfm4-CreER^{T2}* and *Lgr5-CreER^{T2}*. Similar to our findings with *Villin-CreER^{T2}*

(P) Schematic of organoid formation assay to test stem cell activity in non-irradiated *Villin-CreER^{T2}* mice. Duodenal crypts were isolated from TX- or VEH-treated mice and plated in Matrigel to form organoids.

(Q and R) Bright-field images of organoids 3 days post establishment from crypts isolated from (Q) VEH-treated or (R) TX-treated *Villin-CreER^{T2}* mice.

(S) Organoid-forming efficiency was determined by counting organoid number and presented as percent of the number plated (n = 3 mice/group with three technical replicates per mouse).

Quantitative data are presented as means ± SEM (*$p < 0.05$, **$p < 0.01$, $^{\#}p < 0.0001$ TX versus VEH by Student's t test). Scale bars, 100 μm (duodenum) and 250 μm (organoids). See also Figures S1 and S2.

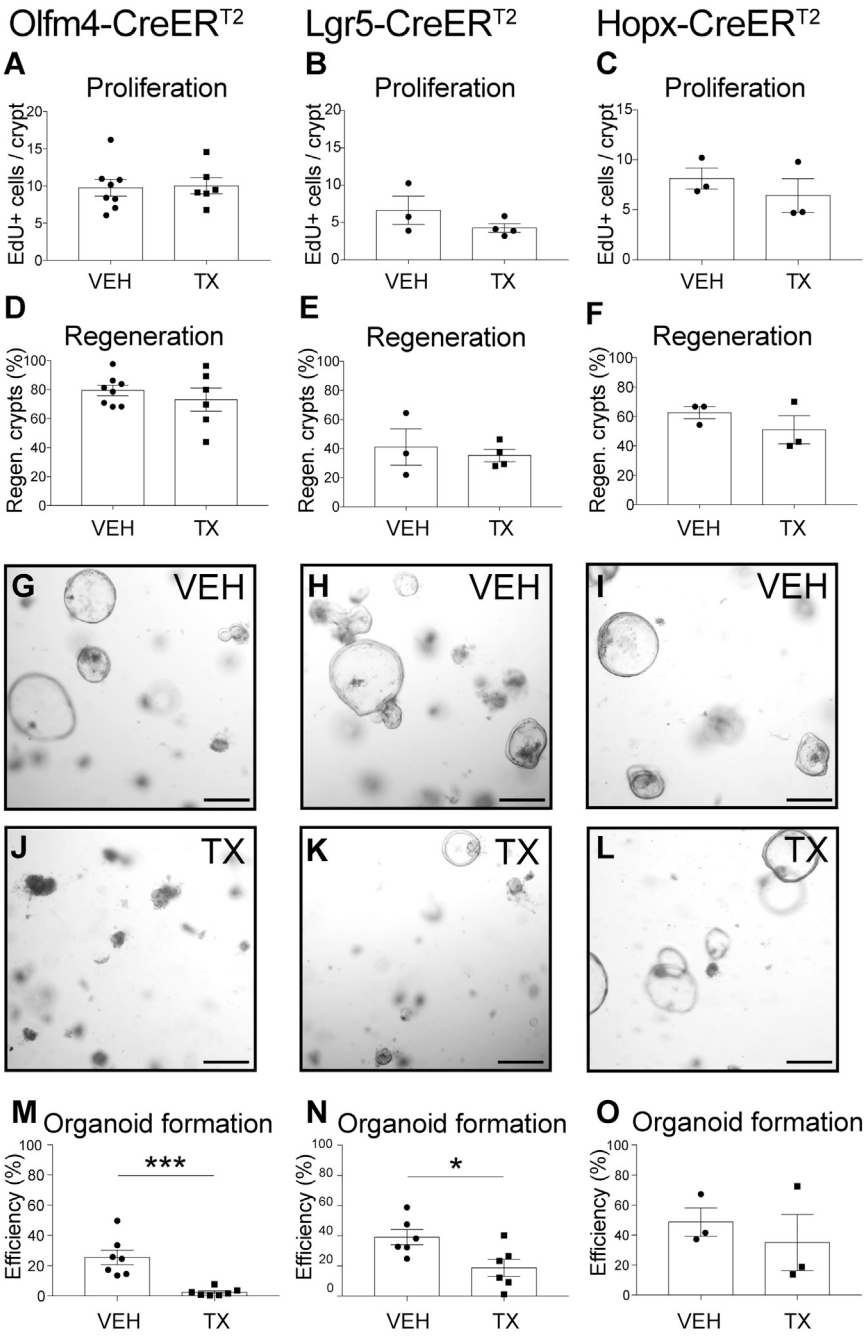

Figure 2. Reduced Organoid-Forming Efficiency after CreER^{T2} Activation in Intestinal Stem Cells

Mouse strains with TX-inducible CreER^{T2} drivers specific for CBC (*Olfm4-CreER^{T2}* and *Lgr5-CreER^{T2}*) or facultative (*Hopx-CreER^{T2}*) ISCs were tested for (A–C) proliferation and (D–F) crypt regeneration after irradiation, or for (G–O) organoid-forming efficiency in non-irradiated mice. (A–F) Mice were treated with TX or VEH daily for 5 days, irradiated a day later, and tissue was collected 3 DPI. (A–C) Cellular proliferation and (D–F) crypt regeneration were quantified (n = 3–8 mice/group). (G–O) Organoids were established from duodenal crypts 1 day after TX- or VEH-treatment, imaged and counted at 3 days post establishment (n = 3–7 mice/group with three technical replicates per mouse).

Quantitative data are presented as means ± SEM (*p < 0.05, ***p < 0.001 TX versus VEH by Student's t test). See also Figures S1 and S3.

mice, TX-treated *Olfm4-CreER^{T2}* mice had normal intestinal histology and proliferation under basal conditions (Figures S1F–S1J). In contrast to the delayed regenerative response in TX-treated *Villin-CreER^{T2}* mice, we observed normal responses to irradiation in TX-treated *Olfm4-CreER^{T2}* and *Lgr5-CreER^{T2}* mice, with cellular proliferation and crypt regeneration at 3 DPI similar to VEH-treated controls (Figures 2A, 2B, 2D, 2E, and S3A–S3F). However, organoid-forming activity was reduced in both strains after TX treatment, similar to *Villin-CreER^{T2}* (Figures 2G, 2H, 2J, and 2K). TX treatment resulted in 10-fold fewer organoids in *Olfm4-CreER^{T2}* and 2-fold fewer organoids in *Lgr5-CreER^{T2}* (Figures 2M and 2N). The results suggest that actively cycling, CBC ISCs are sensitive to CreER^{T2} activation, leading to impaired ISC function.

We also tested one CreER strain that targets a facultative stem cell (FSC) population, *HopX-CreER^{T2}* (Takeda et al., 2011). The expression of this Cre driver is limited to very

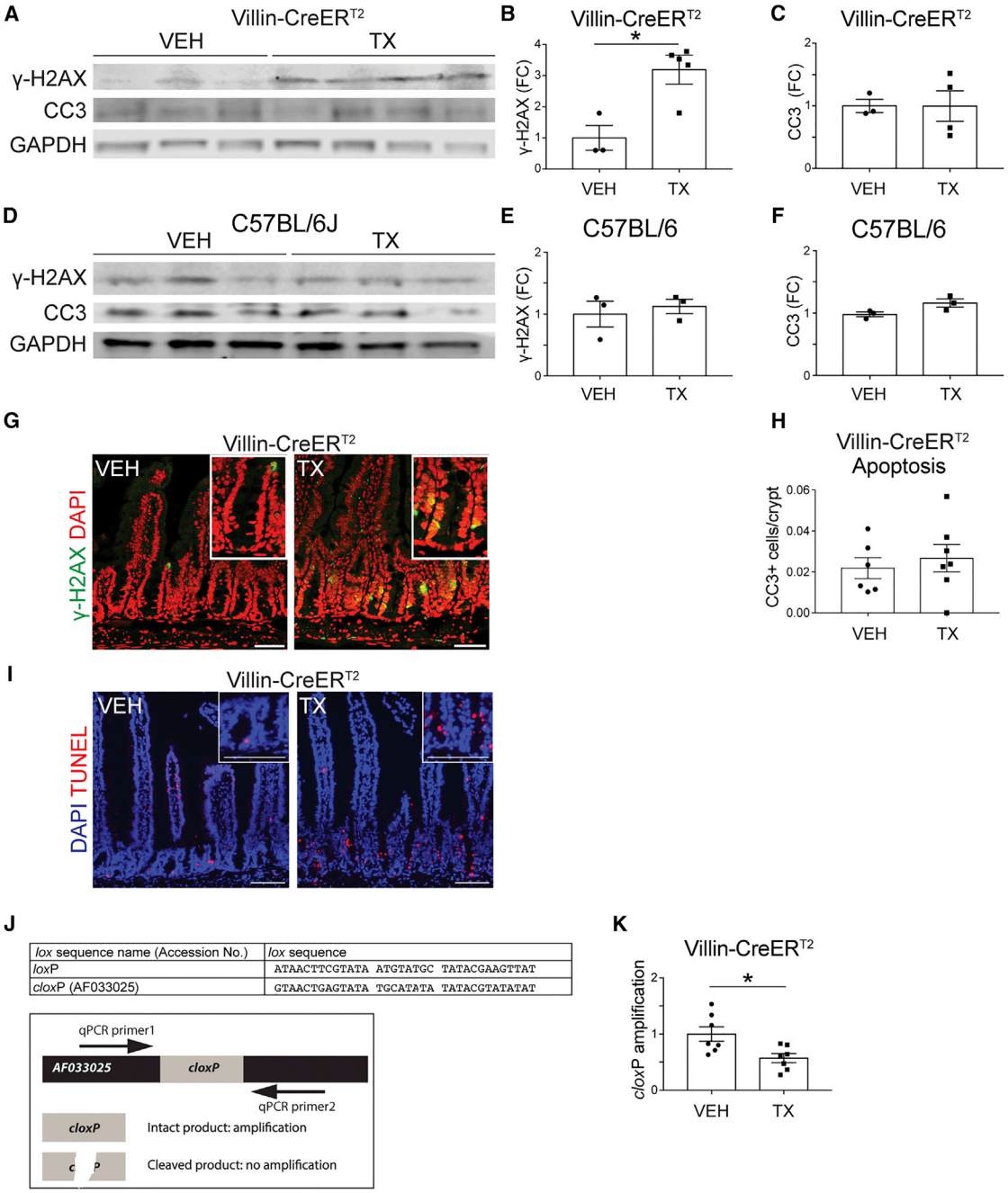

Figure 3. *Villin-CreER^{T2}* Activation Induces DNA Cleavage at *cloxP* Sites

Villin-CreER^{T2} or C57BL/6 mice were treated with VEH or TX daily for 5 days and intestinal crypts were collected 1 day following the last injection.

(A and D) Western blots probing for γ-H2AX, cleaved caspase-3 (CC3), and loading control GAPDH were generated from duodenal crypt lysates prepared from (A) *Villin-CreER^{T2}* or (D) C57BL/6 mice treated with VEH or TX.

(B, C, E, and F) γ-H2AX (B and E) and CC3 (C and F) band signals were quantified and are displayed as means ± SEM (n = 3–4 mice/group; *$p < 0.05$ by Student's t test).

(G and I) Immunofluorescent images of (G) γ-H2AX- and (I) TUNEL-stained VEH- or TX-treated *Villin-CreER^{T2}* duodenum at 1 day post treatment.

(H) Quantified CC3-positive cells per crypt from *Villin-CreER^{T2}* mice 1 day post treatment.

(legend continued on next page)

few cells in the crypt, which can participate in crypt regeneration after γ-irradiation (Li et al., 2016). In contrast to toxicity observed after TX activation of CreER^{T2} in CBCs, the response to radiation, and organoid-forming ability were unchanged in *HopX-CreER^{T2}* mice (Figures 2C, 2F, 2I, 2L, 2O, and S3G–S3I).

CreER^{T2} Activates DNA Cleavage at c*loxP* Sites

We next considered the mechanism by which CreER^{T2} activation leads to impaired ISC function. We posited that TX-mediated CreER^{T2} nuclear translocation induces DNA cleavage. To test this, we performed western blotting for γ-H2AX, which marks DNA DSBs (Kuo and Yang, 2008) and observed a 3-fold increase in the crypts of TX-treated *Villin-CreER^{T2}* mice compared with controls (Figures 3A and 3B). Analysis of C57BL/6 mice showed no differences in γ-H2AX levels between TX- and VEH-treated mice, again demonstrating that the effect is due to activation of CreER^{T2} and not to TX toxicity (Figures 3D and 3E). We also saw increased γ-H2AX staining in cells at the crypt base (Figure 3G). In agreement, TUNEL staining mirrored the γ-H2AX results, demonstrating increased DNA damage (Figure 3I).

To determine whether TX-treated *Villin-CreER^{T2}* mice exhibited DNA damage-induced programmed cell death, we immunoblotted for the apoptotic marker cleaved caspase-3 and found levels to be unchanged in both TX-treated *Villin-CreER^{T2}* and C57BL/6 mice (Figures 3A, 3C, 3D, and 3F). We also confirmed these results by quantifying the number of cleaved caspase-3-positive cells per crypt in tissue sections, showing that induction of DSBs did not induce apoptosis (Figure 3H). The findings suggest that *Villin-CreER^{T2}* activation results in increased DNA cleavage without inducing apoptosis. This agrees with our results showing no obvious histological changes to the duodenum following TX activation under basal conditions (Figures S1A–S1E).

We tested whether activated CreER^{T2} might induce DNA damage by inappropriately targeting regions in the mouse genome with sequence similarity to *loxP*. We designed real-time qPCR primers around the locus of a c*loxP* site (accession number AF033025) previously reported to serve as an active site for Cre recombinase (Thyagarajan et al., 2000). We assessed the integrity of this genomic region following CreER^{T2} activation by comparing amplification from crypt cell DNA isolated from TX- and VEH-treated *Villin-CreER^{T2}* mice (Figure 3J). Real-time qPCR analysis revealed that TX-treated duodenal *Villin-CreER^{T2}* crypt DNA had reduced amplification of this genomic region compared with VEH-treated controls, indicating reduced concentration of this c*loxP* site in the genome (Figure 3K). These results demonstrate that TX-mediated translocation of CreER^{T2} to the nucleus is associated with illegitimate DNA cleavage at a c*loxP* site.

Resolution of CreER^{T2}-Induced ISC Genotoxicity

Understanding the value of the inducible *Villin-CreER^{T2}* mouse strain for genetic analysis of mammalian ISC function, we investigated three methods to minimize ISC toxicity. The first, termed "delayed," involved postponing intestinal challenge for 1 week after the final TX injection (Figures 4A–4J). Analysis of body weight after irradiation showed similar profiles in TX- and VEH-treated mice (Figure 4A). Analysis of intestinal regeneration at 3 and 5 DPI revealed no changes to intestinal histology, including cellular proliferation, crypt regeneration, and villus height (Figures 4B–4J).

Further evidence in support of a delay resolving the *Villin-CreER^{T2}* genotoxicity was shown by normal levels of γ-H2AX and cleaved caspase-3 in the duodenal crypts of *Villin-CreER^{T2}* mice isolated 7 days following the final TX or VEH injection (Figures 4K–4M). Similarly, crypt DNA isolated from TX-treated *Villin-CreER^{T2}* mice 7 days following the final injection had normal c*loxP* amplification (Figure 4N). Further, TUNEL labeling was similar between VEH- and TX-treated *Villin-CreER^{T2}* animals with delay (Figure 4O). Finally, duodenal crypts isolated 7 days following treatment showed normal organoid-forming efficiency (Figure 4P). Similar findings were observed for the CBC-specific *Olfm4-CreER^{T2}* mouse (Figures S4E–S4H; compare Figure S4D with Figure 2M).

We investigated two additional methods of administering TX: daily administration of a lower TX dose (50 mg/kg) over 5 days (5 × 50; Figures 4Q and 4R), and administration of a single 100-mg/kg dose of TX (1 × 100; Figures 4S and 4T), with tissue harvest 1 day later. The results revealed a modest increase in DSBs, as observed by TUNEL staining, in the 5 × 50 experimental paradigm (Figure 4Q) together with a significant decrease in organoid-forming efficiency (Figure 4R). In contrast, we did not observe TX-mediated CreER^{T2} toxicity in the 1 × 100 experiment (Figures 4S and 4T). Thus, we have shown that genotoxicity is dose and time dependent, and identified two methods that minimize damage by reducing the TX dose (1 × 100) or building in a delay after TX treatment.

(J) Known *loxP* sequence compared with the reported c*loxP* AF033025 site (GenBank). Schematic of the qPCR assay designed to measure the amount of intact c*loxP* genomic DNA.
(K) qPCR results from c*loxP* assay normalized to *Gapdh* (n = 3–6 mice/group; *p < 0.05, by Student's t test).
Scale bars, 50 μm. See also Figure S4.

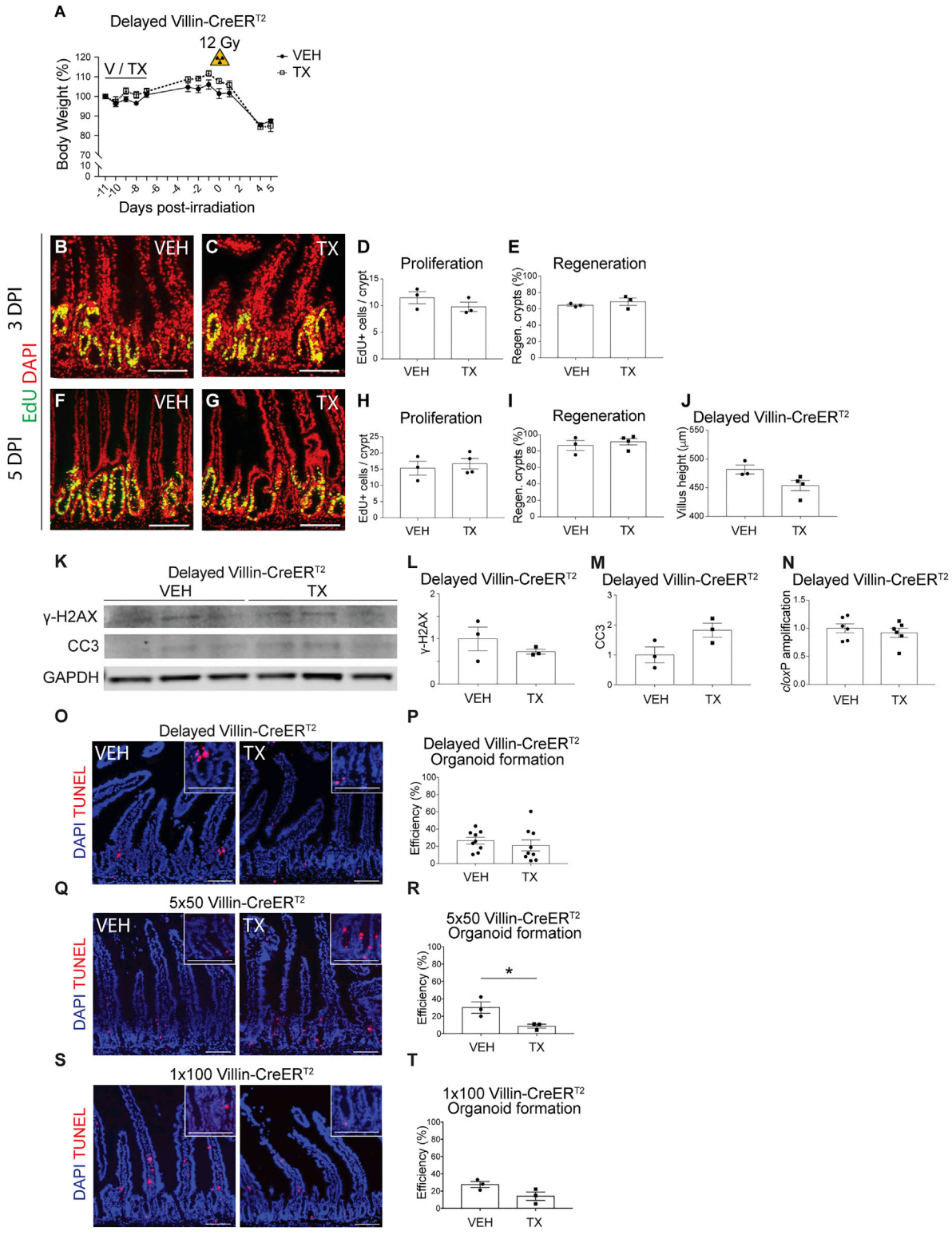

Figure 4. *Villin-CreER^{T2}* Toxicity Is Mitigated by Delay and Reduced TX Dose

(A) Body weight data from *Villin-CreER^{T2}* mice treated with VEH or TX daily for 5 days, followed by γ-irradiation after a 7-day delay (n = 3–4 mice/group).

(legend continued on next page)

DISCUSSION

Our study shows that intestine-specific CreER^{T2} drivers promote illegitimate DNA cleavage events at c*loxP* sites and markedly diminish CBC ISC function. TX activation of the widely used *Villin-CreER^{T2}* resulted in delayed crypt regeneration after epithelial cell damage induced by γ-irradiation. The intestine normally has a remarkable regenerative capacity, with ISC replacement and crypt repair completed within a week after almost complete elimination of the proliferating crypt compartment with 12 Gy whole-body γ-irradiation (Kim et al., 2017). TX-treated *Villin-CreER^{T2}* mice exhibited enhanced weight loss and a delay in crypt regeneration after irradiation, in comparison with VEH-treated *Villin-CreER^{T2}* controls. The regenerative defect suggested a mechanism of ISC toxicity, which was confirmed by loss of organoid-forming activity in TX-treated CreER^{T2} mouse strains. Impaired organoid formation was observed in *Villin-CreER^{T2}* mice, a strain with broad CreER^{T2} expression in all intestinal epithelial cells, as well as two strains with expression limited to CBC ISCs, *Olfm4-CreER^{T2}* and *Lgr5-CreER^{T2}*. These CreER^{T2} driver strains have been extensively used for studies of ISC function, including analysis of mechanisms regulating crypt regeneration after irradiation injury, and ISC activity by measurement of organoid-forming potential.

While we observed changes to both crypt regeneration and organoid-forming efficiency in TX-treated *Villin-CreER^{T2}* mice, we were surprised that TX-treated *Olfm4-CreER^{T2}* and *Lgr5-CreER^{T2}* mice had impaired organoid-forming efficiency but normal regenerative responses. Administration of γ-irradiation doses above 10 Gy has been shown to induce loss of CBC ISCs through apoptosis (Potten, 2004; Wang et al., 2015). Normal regeneration in *Olfm4-CreER^{T2}* and *Lgr5-CreER^{T2}* mice suggests that the effect observed in *Villin-CreER^{T2}* animals may not be solely caused by CreER^{T2} activation in CBCs. Rather, the delayed regenerative response could be a result of CreER^{T2}-induced damage to FSCs, which are mobilized to repair the crypts following CBC loss (Roche et al., 2015; Takeda et al., 2011; Tian et al., 2011; Yan et al., 2012). FSCs are also thought to contribute to organoid formation. This led to our analysis of the *HopX-CreER^{T2}* mouse strain, which activates CreER^{T2} in a small subset of FSCs (Takeda et al., 2011). This strain showed no effect on intestinal regeneration or organoid formation following TX administration. This may reflect the small number of crypt cells targeted by *HopX-CreER^{T2}*. A rigorous interrogation of CreER^{T2} mouse strains with different coverage of FSCs may be warranted (e.g., *Bmi1-CreER^{T2}* and *Sox9-CreER^{T2}*). An additional possibility for our *HopX-CreER^{T2}* results may be the different sensitivities of CreER^{T2} activation in FSCs versus CBC stem cell populations. The susceptibility of various crypt cell populations to CreER^{T2}-induced genotoxicity warrants further study.

The *Villin-CreER^{T2}* and *Lgr5-CreER^{T2}* mouse strains are commonly used, with hundreds of published studies employing these Cre drivers to manipulate genes for analysis of intestinal development, physiology, and pathophysiology. In particular, these strains have been important to study ISC function. The genotoxicity and ISC defects uncovered in our study are a serious consideration for studies that employ these, or other Cre drivers, expressed in the intestinal crypt.

Mouse studies using Cre recombinase have become a mainstay for analysis of gene function *in vivo*. It is commonly assumed that Cre activation per se does not induce adverse events. However, Cre-mediated cellular toxicity resulting from illegitimate DNA cleavage at c*loxP* sites has been previously observed in cultured cells and mouse tissues (Loonstra et al., 2001; Schmidt et al., 2000; Silver and Livingston, 2001; Thyagarajan et al., 2000). Cre-mediated genotoxicity appears to be dosage dependent, and proliferating cells seemingly exhibit enhanced sensitivity (Higashi et al., 2009; Loonstra et al., 2001; Naiche and Papaioannou, 2007; Schmidt et al., 2000), which would predict that proliferating stem and progenitor cells would be particularly sensitive to Cre-mediated toxicity. However, few studies have examined adult stem cell toxicity after CreER^{T2} activation *in vivo*. Our finding of CreER^{T2}-induced ISC toxicity would prompt stem cell biologists studying other adult stem cell populations to be cautious when activating CreER^{T2} alleles. Careful experimental design must include the proper controls to rule out

(B–J) EdU-stained duodenal tissue sections (B, C, F, and G) at 3DPI (B and C) and 5 DPI (F and G). (D and H) Proliferation, (E and I) regenerating crypts, and (J) villus height were quantified.
(K) Western blot analysis probing for γ-H2AX, CC3, and GAPDH, using duodenal crypt lysates from *Villin-CreER^{T2}* mice 7 days post treatment.
(L and M) γ-H2AX (L) and CC3 (M) band signals were quantified and are displayed as means ± SEM (n = 3 mice/group).
(N–T) qPCR gene amplification of c*loxP* normalized to *Gapdh* (N) (n = 6 mice/group). TUNEL staining of duodenum of non-irradiated (O) "delayed" VEH- or TX-treated *Villin-CreER^{T2}* mice, (Q) *Villin-CreER^{T2}* mice administered five daily doses of 50 mg/kg TX and analyzed 1 day later (5 × 50), and (S) *Villin-CreER^{T2}* mice administered a single dose of 100 mg/kg TX and analyzed 1 day later (1 × 100). Organoid-forming efficiency was also determined for (P) delayed, (R) 5 × 50, and (T) 1 × 100 VEH- and TX-treated *Villin-CreER^{T2}* mice (n = 3–9 mice/group with three technical replicates per mouse.
*p < 0.05 by Student's t test). Scale bars, 100 μm. See also Figure S4.

Cre-mediated genotoxicity as a potential cause of stem cell phenotypes induced in studies using CreER mouse strains.

EXPERIMENTAL PROCEDURES

A detailed description of all methods is included in Supplemental Information.

Animal Treatment

Mouse use was approved by the Institutional Animal Care & Use Committee at the University of Michigan. To activate CreER^{T2}-mediated recombination, mice were injected intraperitoneally with TX (50 or 100 mg/kg; 10 mg/mL in 5% ethanol and 95% corn oil; Sigma) or VEH (5% ethanol, 95% corn oil) once per day for 1 or 5 days, and tissue was collected as indicated. To induce intestinal injury, mice were exposed to one dose of 12 Gy whole-body irradiation from a ^{137}Cs source. Animals were injected intraperitoneally with 5-ethynyl-2′-deoxyuridine (EdU) (25 mg/kg; Life Technologies) 2 hr prior to tissue collection.

Immunohistochemistry

Duodenal paraffin sections (5 μm) were stained with H&E to analyze intestinal morphology. Villus height was determined by measuring from the tip of intact villi to the top shoulder of adjacent crypts using ImageJ software (1.52a; Wayne Rasband, NIH). The number of EdU-positive cells was counted from well-oriented crypts, identified from images obtained from adjacent H&E-stained sections. Regeneration was assessed using the adapted crypt microcolony survival assay method (Cohn et al., 1997). Regenerating crypts were measured as the number of well-oriented crypts with four or more EdU-positive cells divided by the total number of well-oriented crypts.

Gene Integrity Analysis

For quantification of *cloxP* amplification, DNA from duodenal crypts was extracted using the Easy-DNA kit (Invitrogen, K1800-01). qPCR assays for *cloxP* were run in triplicate, and normalized to *Gapdh* as an internal control.

SUPPLEMENTAL INFORMATION

Supplemental Information includes Supplemental Experimental Procedures and four figures and can be found with this article online at https://doi.org/10.1016/j.stemcr.2018.10.014.

AUTHOR CONTRIBUTIONS

N.B. and L.C.S. designed the project. N.B. and E.A.C. performed the experiments. N.B. and L.C.S. interpreted the data and wrote the manuscript. E.A.C. provided critical feedback.

ACKNOWLEDGMENTS

We thank Dr. Ivan Maillard, whose insightful questions led to the conception of the project, Yasmine Abushukur and Theresa Keeley for technical help, Erin Collin for maintaining the mouse colony, and the Nusrat/Parkos lab for the gift of the *Villin-Cre* mice and for supplementing our *Villin-CreER^{T2}* mouse stores. N.B. was supported by the Cellular and Molecular Biology program, a Rackham research grant, and the Benard L. Maas Fellowship. The research was funded by NIH R01-DK096972 (to L.C.S.), and Core support from the Michigan Gastrointestinal Research Center Grant NIH P30-DK34933.

Received: July 8, 2018
Revised: October 15, 2018
Accepted: October 17, 2018
Published: November 15, 2018

REFERENCES

Barker, N., van Es, J.H., Kuipers, J., Kujala, P., van den Born, M., Cozijnsen, M., Haegebarth, A., Korving, J., Begthel, H., Peters, P.J., et al. (2007). Identification of stem cells in small intestine and colon by marker gene Lgr5. Nature *449*, 1003–1007.

Bouabe, H., and Okkenhaug, K. (2013). Gene targeting in mice: a review. Methods Mol. Biol. *1064*, 315–336.

Cohn, S.M., Schloemann, S., Tessner, T., Seibert, K., and Stenson, W.F. (1997). Crypt stem cell survival in the mouse intestinal epithelium is regulated by prostaglandins synthesized through cyclooxygenase-1. J. Clin. Invest. *99*, 1367–1379.

Higashi, A.Y., Ikawa, T., Muramatsu, M., Economides, A.N., Niwa, A., Okuda, T., Murphy, A.J., Rojas, J., Heike, T., Nakahata, T., et al. (2009). Direct hematological toxicity and illegitimate chromosomal recombination caused by the systemic activation of CreERT2. J. Immunol. *182*, 5633–5640.

Huh, W.J., Mysorekar, I.U., and Mills, J.C. (2010). Inducible activation of Cre recombinase in adult mice causes gastric epithelial atrophy, metaplasia, and regenerative changes in the absence of "floxed" alleles. Am. J. Physiol. Gastrointest. Liver Physiol. *299*, G368–G380.

Huh, W.J., Khurana, S.S., Geahlen, J.H., Kohli, K., Waller, R.A., and Mills, J.C. (2012). Tamoxifen induces rapid, reversible atrophy, and metaplasia in mouse stomach. Gastroenterology *142*, 21–24.e7.

Kim, C.-K., Yang, V.W., and Bialkowska, A.B. (2017). The role of intestinal stem cells in epithelial regeneration following radiation-induced gut injury. Curr. Stem Cell Reports *3*, 320–332.

Kuo, L.J., and Yang, L.-X. (2008). Gamma-H2AX - a novel biomarker for DNA double-strand breaks. In Vivo *22*, 305–309.

Li, N., Nakauka-Ddamba, A., Tobias, J., Jensen, S.T., and Lengner, C.J. (2016). Mouse label-retaining cells are molecularly and functionally distinct from reserve intestinal stem cells. Gastroenterology *151*, 298–310.e7.

Loonstra, A., Vooijs, M., Beverloo, H.B., Allak, B.A., van Drunen, E., Kanaar, R., Berns, A., and Jonkers, J. (2001). Growth inhibition and DNA damage induced by Cre recombinase in mammalian cells. Proc. Natl. Acad. Sci. U S A *98*, 9209–9214.

Madison, B.B., Dunbar, L., Qiao, X.T., Braunstein, K., Braunstein, E., and Gumucio, D.L. (2002). Cis elements of the villin gene control expression in restricted domains of the vertical (crypt) and horizontal (duodenum, cecum) axes of the intestine. J. Biol. Chem. *277*, 33275–33283.

el Marjou, F., Janssen, K.-P., Chang, B.H.-J., Li, M., Hindie, V., Chan, L., Louvard, D., Chambon, P., Metzger, D., and Robine, S. (2004).

Tissue-specific and inducible Cre-mediated recombination in the gut epithelium. Genesis *39*, 186–193.

Metzger, D., Clifford, J., Chiba, H., and Chambon, P. (1995). Conditional site-specific recombination in mammalian cells using a ligand-dependent chimeric Cre recombinase. Proc. Natl. Acad. Sci. U S A *92*, 6991–6995.

Naiche, L.A., and Papaioannou, V.E. (2007). Cre activity causes widespread apoptosis and lethal anemia during embryonic development. Genesis *45*, 768–775.

Potten, C.S. (2004). Radiation, the ideal cytotoxic agent for studying the cell biology of tissues such as the small intestine. Radiat. Res. *161*, 123–136.

Roche, K.C., Gracz, A.D., Liu, X.F., Newton, V., Akiyama, H., and Magness, S.T. (2015). SOX9 maintains reserve stem cells and preserves radioresistance in mouse small intestine. Gastroenterology *149*, 1553–1563.e10.

Schmidt, E.E., Taylor, D.S., Prigge, J.R., Barnett, S., and Capecchi, M.R. (2000). Illegitimate Cre-dependent chromosome rearrangements in transgenic mouse spermatids. Proc. Natl. Acad. Sci. U S A *97*, 13702–13707.

Schuijers, J., van der Flier, L.G., van Es, J., and Clevers, H. (2014). Robust cre-mediated recombination in small intestinal stem cells utilizing the olfm4 locus. Stem Cell Reports *3*, 234–241.

Silver, D.P., and Livingston, D.M. (2001). Self-excising retroviral vectors encoding the Cre recombinase overcome Cre-mediated cellular toxicity. Mol. Cell *8*, 233–243.

Takeda, N., Jain, R., LeBoeuf, M.R., Wang, Q., Lu, M.M., and Epstein, J.A. (2011). Interconversion between intestinal stem cell populations in distinct niches. Science *334*, 1420–1424.

Thyagarajan, B., Guimarães, M.J., Groth, A.C., and Calos, M.P. (2000). Mammalian genomes contain active recombinase recognition sites. Gene *244*, 47–54.

Tian, H., Biehs, B., Warming, S., Leong, K.G., Rangell, L., Klein, O.D., and de Sauvage, F.J. (2011). A reserve stem cell population in small intestine renders Lgr5-positive cells dispensable. Nature *478*, 255–259.

Wang, X., Wei, L., Cramer, J.M., Leibowitz, B.J., Judge, C., Epperly, M., Greenberger, J., Wang, F., Li, L., Stelzner, M.G., et al. (2015). Pharmacologically blocking p53-dependent apoptosis protects intestinal stem cells and mice from radiation. Sci. Rep. *5*, 8566.

Yan, K.S., Chia, L.A., Li, X., Ootani, A., Su, J., Lee, J.Y., Su, N., Luo, Y., Heilshorn, S.C., Amieva, M.R., et al. (2012). The intestinal stem cell markers Bmi1 and Lgr5 identify two functionally distinct populations. Proc. Natl. Acad. Sci. U S A *109*, 466–471.

Zhu, Y., Huang, Y.-F., Kek, C., and Bulavin, D.V. (2013). Apoptosis differently affects lineage tracing of Lgr5 and Bmi1 intestinal stem cell populations. Cell Stem Cell *12*, 298–303.

Stem Cell Reports, Volume *11*

Supplemental Information

Genome Toxicity and Impaired Stem Cell Function after Conditional Activation of CreER^{T2} in the Intestine

Natacha Bohin, Elizabeth A. Carlson, and Linda C. Samuelson

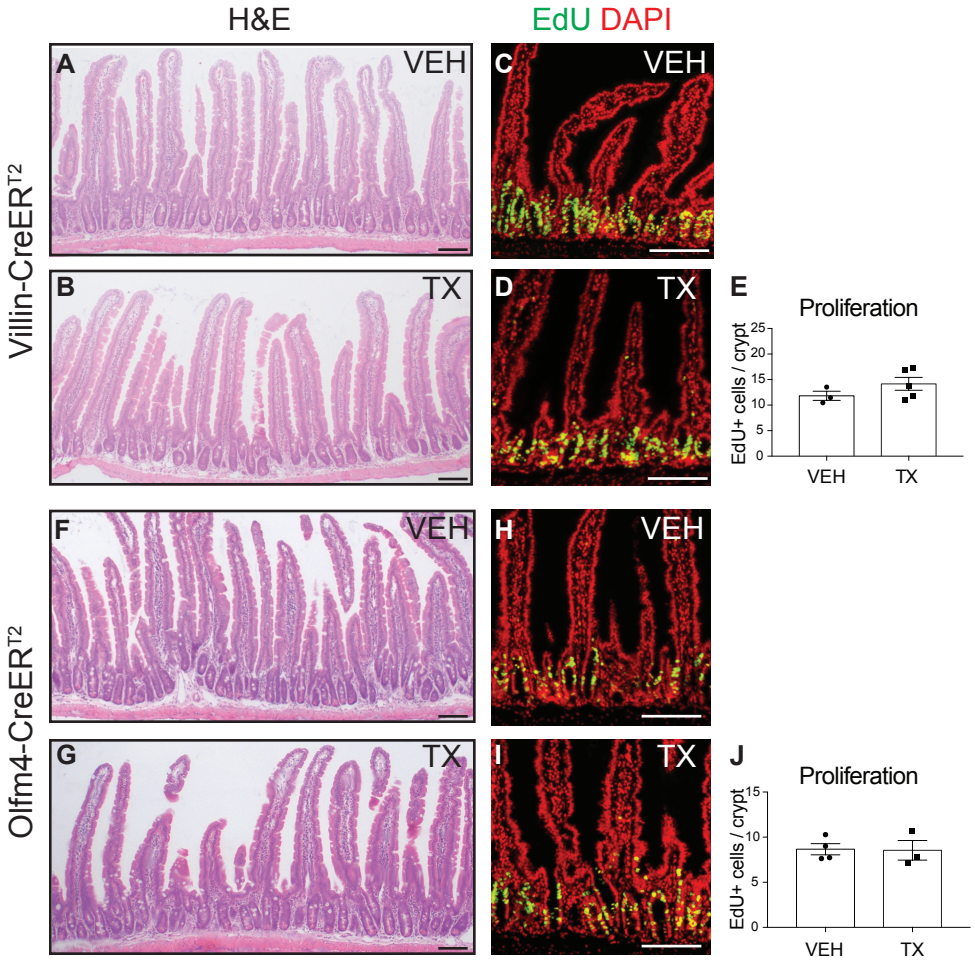

Figure S1. Normal intestinal histology in tamoxifen-treated *Villin-CreER^{T2}* and *Olfm4-CreER^{T2}* mice. Related to Figures 1 and 2.

Villin-CreER^{T2} and *Olfm4-CreER^{T2}* mice were treated with tamoxifen (TX; 100 mg/kg) or vehicle (VEH) daily for 5 days, and intestinal tissue was collected 1 day following the final injection. Duodenal histology was assessed by (A-B, F-G) H&E staining. (C-E, H-J) Cellular proliferation was assessed by EdU incorporation. Proliferating cells are presented as the number of EdU-positive cells per crypt (mean +/- SEM, n=3-5 mice/group).

Scale bars = 100µm.

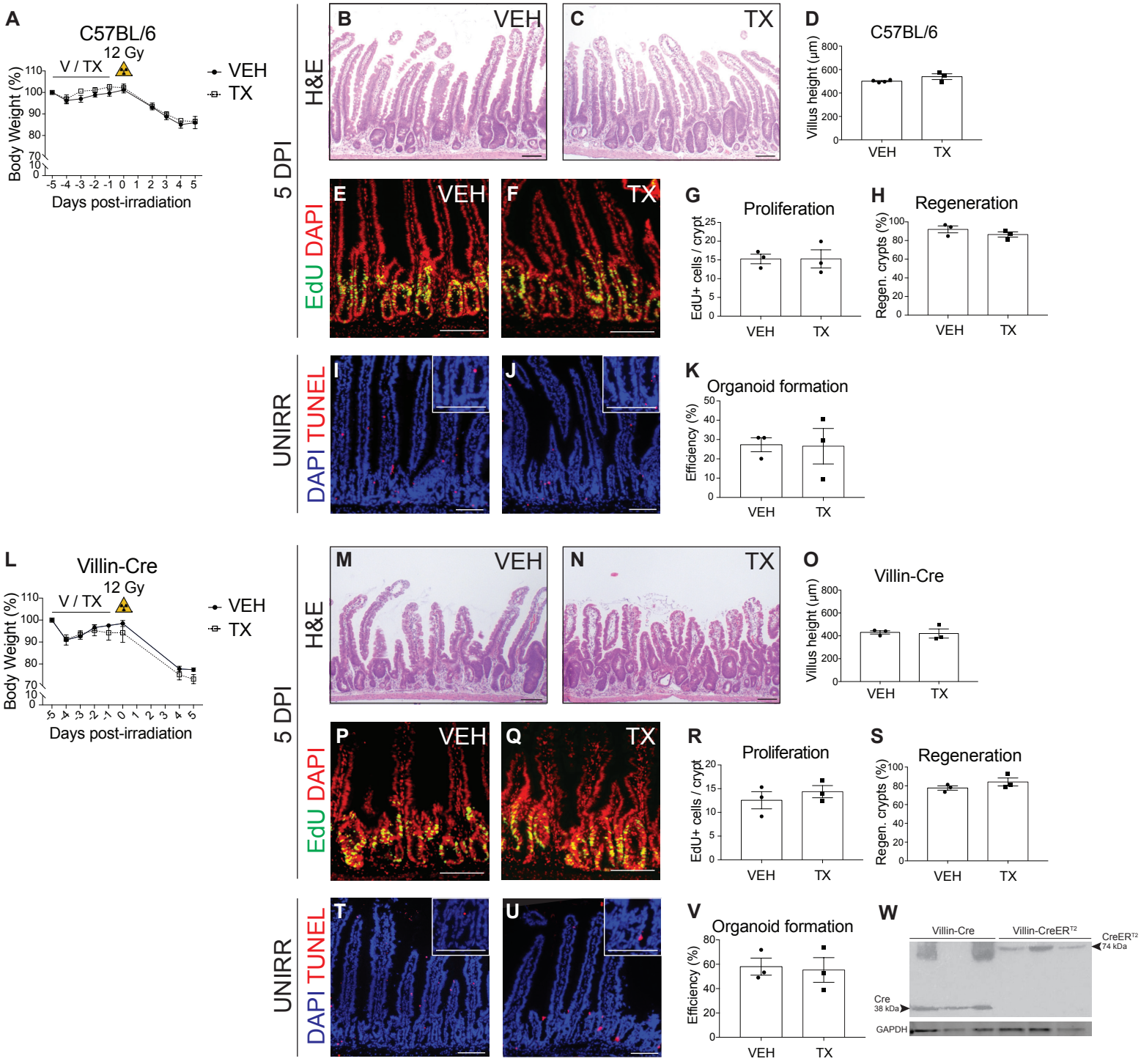

Figure S2. Normal intestinal regeneration and organoid formation in tamoxifen-treated C57BL/6 and *Villin-Cre* mice. Related to Figure 1.

(A-H) C57BL/6 and (L-S) *Villin-Cre* mice were treated with TX or VEH daily for 5 days, irradiated (12Gy) 1 day later, and intestinal tissue was collected at 5 DPI.

(A, L) Mouse body weight relative to weight at the initiation of treatment is presented as mean +/- SEM (n=3-6 mice/group). Duodenal crypt regeneration post-irradiation was assessed by (B-C, M-N) H&E staining and (E-F, P-Q) EdU incorporation.

(D, O) Villus height measurements presented as mean +/- SEM (n=3-4 mice/group).

(G, R) Proliferating cells are presented as the number of EdU-positive cells per crypt.

(H, S) Regenerating crypts were defined as intact crypts with 4 or more EdU-positive cells and presented as percent of the total crypts. Quantitative data are presented as mean +/- SEM (n=3 mice/group).

(I-J, T-U) TUNEL staining of unirradiated (UNIRR) TX- and VEH-treated C57BL/6 and *Villin-Cre* mice 24h following the last day of injection.

(K, V) C57BL/6 and *Villin-Cre* duodenal crypts were isolated from UNIRR TX- or VEH-treated mice and plated (200 crypts/well) to form organoids. Organoid formation efficiency is presented as mean +/- SEM (n=3 mice/group with 3 technical replicates per mouse).

(W) Western blot probing for Cre, and loading control GAPDH in duodenal crypt lysates of *Villin-Cre* and *Villin-CreER^{T2}* mice.

Duodenum images scale bars = 100µm.

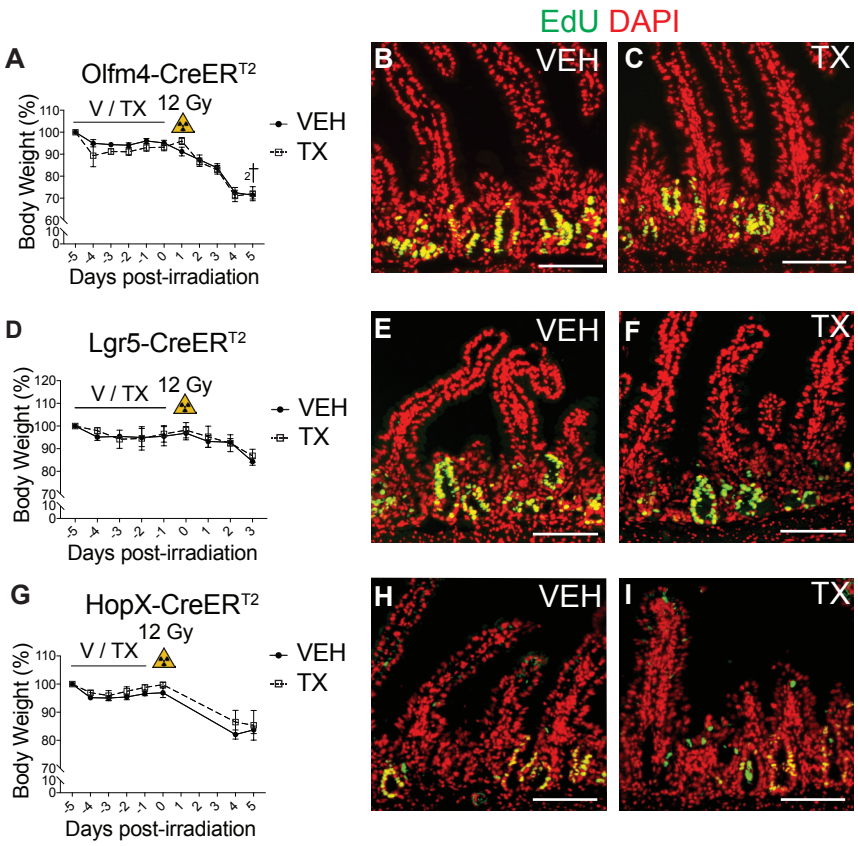

Figure S3. Normal post-irradiation regenerative responses after CreER^{T2} activation in intestinal stem cells. Related to Figure 2.
Mouse strains with TX-inducible CreER^{T2} drivers specific for active (*Olfm4-CreER^{T2}* and *Lgr5-CreER^{T2}*) or facultative (*HopX-CreER^{T2}*) intestinal stem cells were treated with TX or VEH daily for 5 days, irradiated (12Gy) 1 day later and tissue was collected at 3DPI.
(A, D, G) Mouse body weight relative to weight at the initiation of treatment is presented as mean +/- SEM (n=3-14 mice/group).
(B-C, E-F, H-I) Cellular proliferation was assessed by EdU incorporation (n=3-8). Scale bars = 100μm.

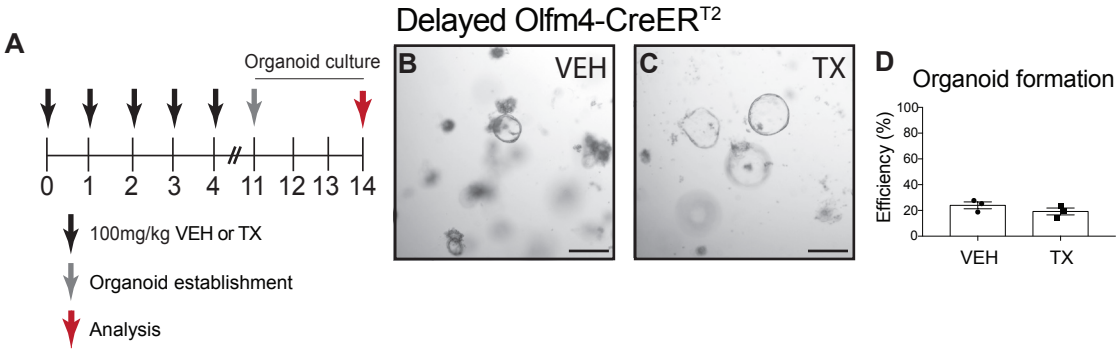

Figure S4. Tamoxifen-induced *Olfm4-CreER^{T2}* toxicity is abated by delay. Related to Figure 4.
(A) Schematic of organoid formation efficiency assay. Organoids were established from duodenal crypts isolated from *Olfm4-CreER^{T2}* mice 7 days after treatment with VEH or TX.
(B,C) Brightfield images of organoids 3 days post-establishment.
(D) Organoid forming efficiency was determined by counting the number of organoids in each well at 3 days post-establishment (n=3 mice/group with 3 technical replicates per mouse).
Scale bars = 250μm.

SUPPLEMENTAL EXPERIMENTAL PROCEDURES

Mice

Mice were housed in ventilated and automated watering cages with a 12-hour light /dark cycle under specific pathogen-free conditions. The following mouse strains were employed: *Villin-CreER^{T2}* (el Marjou et al., 2004), *Villin-Cre* (Madison et al., 2002), *Olfm4-ires-EGFP-CreER^{T2}* (gift from Dr. Hans Clevers) (Schuijers et al., 2014), *Lgr5-EGFP-ires-CreER^{T2}* (JAX strain 008875) (Barker et al., 2007), *HopX-CreER^{T2}* (JAX strain 017606) (Takeda et al., 2011). Mice were maintained on a C57BL/6 strain background. Mice of both sexes aged 1.5-4 months were used.

Tissue collection

Intestinal tissue was harvested following *ad libitum* feeding and fixed in 4% paraformaldehyde in 1X PBS overnight before paraffin processing, as previously described (VanDussen et al., 2012). Intestinal crypts were harvested from duodenum, as previously described (Carulli et al., 2015).

Organoid culture

Mouse intestinal organoid cultures were established from duodenal crypts and maintained as described (Demitrack et al., 2015), with modifications. Longitudinally opened 6 cm of proximal intestinal tissue was washed in ice cold DPBS (Gibco), with antibiotics penicillin-streptomycin (1X) and gentamycin (1X; Gibco) for 20 min, cut into 1 cm pieces, and incubated in 15 mM EDTA in DPBS with antibiotics for 35 min at 4°C on a rocking platform. Tissue was vortexed for 2 min., and the solution was passed through a 70-µm filter. Crypts were gravity settled for 10min, the supernatant was decanted, the remaining pellet was resuspended in 1X DPBS with antibiotics, and centrifuged at 150x*g* for 10 min. The resulting crypt pellet was resuspended in complete culture media [50% L-WRN-conditioned media (Miyoshi and Stappenbeck, 2013), 20% fetal bovine serum (Atlas Biologicals), antibiotics, 2 mM L-glutamine (Gibco), 1X Fungizone (Gibco) and Y- 27632 (10 µM; Tocris) in advanced DMEM/F12 (Gibco)]. To test organoid formation efficiency, 600 crypts (extrapolated by determining crypt number per µL by counting crypts from a 5 µL droplet of crypt suspension) were mixed with 120 µL Matrigel (BD Biosciences), and 40 µL aliquots were plated in pre-warmed 24-well plates. After 30 min at 37°C, 500 µL complete culture media was overlaid. Culture media without Y-27632 was replaced every other day. The efficiency of organoid formation was determined by counting organoids at 3 days following plating, and normalizing to the number of plated crypts.

Immunohistochemistry

Immunostaining with rabbit α-Ki67 (1:200, Thermo Scientific RM-9106), and rabbit α-γ-H2AX (1:50, Cell Signaling 9718) was performed as described (Lopez-Diaz et al., 2006). A goat anti-rabbit IgG Alexa Fluor 488 polyclonal secondary antibody was used (1:400, Invitrogen A27034). EdU-Click-it kit (Life Technologies) was used to identify proliferating cells. Images were captured on a Nikon E800 microscope with Olympus DP controller software, except for γ-H2AX-immunostained images, which were captured on a Leica SP5 inverted confocal microscope with Leica software.

Western Blot Analysis

Isolated duodenal crypts were lysed in RIPA buffer (Thermo, 89900) containing protease and phosphatase inhibitor cocktail (Thermo Scientific, 78440). Cell lysates (40 µg protein) were mixed with NuPAGE LDS Sample Buffer (Thermo, NP0007) and separated by sodium dodecyl sulfate polyacrylamide gel electrophoresis using NuPAGE MOPS SDS Running Buffer (Thermo, NP0001) and NuPAGE 4-12% Bis-Tris gels (Thermo, NP0335), following manufacturer recommendations. Protein transfer onto 0.45µm pore size nitrocellulose membrane (GE Healthcare) at 100V for 45 min preceded blocking in Odyssey Blocking Buffer (Li-COR, 927-40000) for 1 hour at room temperature. Immunoblotting with rabbit α-γ-H2AX (1:50, Cell Signaling 9718), rabbit α-cleaved caspase 3 (1:500, Cell Signaling 9664), and mouse α-GAPDH (1:10,000, Thermo Scientific MA5-15738) was performed on a rocking platform overnight at 4°C. IRDye 800CW Goat α-rabbit (1:10,000, LI-COR 925-32211) and IRDye 680RD Goat α-mouse (1:10,000, LI-COR 925-68070) secondary antibodies were used to visualize probed proteins. Membrane was scanned on an Odyssey Imager (LI-COR). Western blot analysis was performed using the free Image Studio Lite software (LI-COR).

Gene integrity analysis

Quantitative polymerase chain reaction was performed as previously described (Lopez-Diaz et al., 2006), using 40ng DNA and *clox*P primers with sequences: GGT CTG AGC TAT ACT TAC AAA GGT (forward) and GCT ATC

ACA ATG GTG GTC CG (reverse), which yielded a 300 bp amplified product size. Assays for each sample were run in triplicate and normalized to *Gapdh* as an internal control, with primer sequences: TCA AGA AGG TGG TGA AGC AGG (forward) and TAT TAT GGG GGT CTG GGA TGG (reverse), which yielded a 350 bp amplified product size.

Statistical analysis

All experiments were performed with at least 3 biological replicates per group. Quantitative data are presented as mean ± SEM. Comparisons between 2 groups were conducted with unpaired two-tailed Student *t* tests using the Prism software (Graphpad). Significance is reported as * ($P<0.05$), ** ($P<0.01$), *** ($P<0.001$), and $^{\#}$ ($P<0.0001$).

SUPPLEMENTAL REFERENCES

Barker, N., van Es, J.H., Kuipers, J., Kujala, P., van den Born, M., Cozijnsen, M., Haegebarth, A., Korving, J., Begthel, H., Peters, P.J., et al. (2007). Identification of stem cells in small intestine and colon by marker gene Lgr5. Nature *449*, 1003–1007.

Carulli, A.J., Keeley, T.M., Demitrack, E.S., Chung, J., Maillard, I., and Samuelson, L.C. (2015). Notch receptor regulation of intestinal stem cell homeostasis and crypt regeneration. Dev. Biol. *402*, 98–108.

Demitrack, E.S., Gifford, G.B., Keeley, T.M., Carulli, A.J., VanDussen, K.L., Thomas, D., Giordano, T.J., Liu, Z., Kopan, R., and Samuelson, L.C. (2015). Notch signaling regulates gastric antral LGR5 stem cell function. EMBO J. *34*, 2522–2536.

Lopez-Diaz, L., Hinkle, K.L., Jain, R.N., Zavros, Y., Brunkan, C.S., Keeley, T., Eaton, K.A., Merchant, J.L., Chew, C.S., and Samuelson, L.C. (2006). Parietal cell hyperstimulation and autoimmune gastritis in cholera toxin transgenic mice. Am. J. Physiol. Liver Physiol. *290*, G970–G979.

el Marjou, F., Janssen, K.-P., Chang, B.H.-J., Li, M., Hindie, V., Chan, L., Louvard, D., Chambon, P., Metzger, D., and Robine, S. (2004). Tissue-specific and inducible Cre-mediated recombination in the gut epithelium. Genesis *39*, 186–193.

Miyoshi, H., and Stappenbeck, T.S. (2013). In vitro expansion and genetic modification of gastrointestinal stem cells in spheroid culture. Nat. Protoc. *8*, 2471–2482.

Schuijers, J., van der Flier, L.G., van Es, J., and Clevers, H. (2014). Robust cre-mediated recombination in small intestinal stem cells utilizing the olfm4 locus. Stem Cell Reports *3*, 234–241.

Takeda, N., Jain, R., LeBoeuf, M.R., Wang, Q., Lu, M.M., and Epstein, J.A. (2011). Interconversion between intestinal stem cell populations in distinct niches. Science *334*, 1420–1424.

VanDussen, K.L., Carulli, A.J., Keeley, T.M., Patel, S.R., Puthoff, B.J., Magness, S.T., Tran, I.T., Maillard, I., Siebel, C., Kolterud, Å., et al. (2012). Notch signaling modulates proliferation and differentiation of intestinal crypt base columnar stem cells. Development *139*, 488–497.